Journal of Human Evolution 61 (2011) 347–362

Contents lists available at ScienceDirect

Journal of Human Evolution

journal homepage: www.elsevier.com/locate/jhevol

Partial skeleton of *Theropithecus brumpti* (Primates, Cercopithecidae) from the Chemeron Formation of the Tugen Hills, Kenya

Christopher C. Gilbert [a,b,c,*], Emily D. Goble [d], John D. Kingston [e], Andrew Hill [d]

[a] Department of Anthropology, Hunter College of the City University of New York, 695 Park Avenue, NY 10021, USA
[b] Department of Anthropology, Graduate Center of the City University of New York, 365 Fifth Avenue, NY 10016, USA
[c] New York Consortium in Evolutionary Primatology, New York, NY, USA
[d] Department of Anthropology, Yale University, PO Box 208277, New Haven, CT 06520-8277, USA
[e] Department of Anthropology, Emory University, 1557 Dickey Drive, Atlanta, GA 30322, USA

ARTICLE INFO

Article history:
Received 27 October 2010
Accepted 21 April 2011

Keywords:
Cercopithecoid
Papionin
Crania
Postcrania
Baboons
Plio-Pleistocene

ABSTRACT

Here we describe a complete skull and partial skeleton of a large cercopithecoid monkey (KNM-TH 46700) discovered in the Chemeron Formation of the Tugen Hills at BPRP Site #152 (2.63 Ma). Associated with the skeleton was a mandible of an infant cercopithecoid (KNM-TH 48364), also described here. KNM-TH 46700 represents an aged adult female of *Theropithecus brumpti*, a successful Pliocene papionin taxon better known from the Omo Shungura Formation in Ethiopia and sites east and west of Lake Turkana, Kenya. While the morphology of male *T. brumpti* is well-documented, including a partial skeleton with both cranial and postcranial material, the female *T. brumpti* morphotype is not well-known. This skeleton represents some of the first associated evidence of cranial and postcranial female *T. brumpti* remains. In addition to the complete skull, postcranial material includes elements of the axial skeleton and lower limb. While aspects of the skeleton conform to those of specimens previously assigned to *T. brumpti*, other features on the femur and tibia appear to differ from those previously described for this species. It is unclear whether these differences represent general variation within the *T. brumpti* population, variation between the sexes in *T. brumpti*, or the incorrect assignment of previous isolated hindlimb specimens. In total, the observable morphological features of the hindlimb suggest that KNM-TH 46700 was a terrestrial quadruped similar to modern savannah baboons (*Papio*). From the available evidence, it is difficult to assess whether or not KNM-TH 46700 frequently engaged in the specialized squatting and shuffling behavior observed in extant geladas (*Theropithecus gelada*).

Introduction

Theropithecus brumpti is a well-known and distinctive fossil papionin commonly found at Turkana Basin paleontological sites from ~3.5 Ma to 2.0 Ma (Leakey, 1993; Jablonski et al., 2008). The species is easily recognized by its remarkable cranium, which is dominated by exceptionally large and flaring zygomatics. While hundreds of *T. brumpti* specimens have been recovered since its initial description (Arambourg, 1947), rarely are cranial and postcranial material found together in association. Even less common is the recovery of a partial or complete skeleton, a phenomenon that is, unfortunately, rare throughout all of paleoanthropology. Well-associated craniodental and skeletal remains are ultimately crucial for comprehensive and accurate interpretations of an extinct species' paleobiology. In this case, accurate interpretations of *T. brumpti*'s locomotor behavior are also potentially important for paleoenvironmental reconstructions.

Previous functional analyses of both associated and unassociated *T. brumpti* postcrania suggest a mix of arboreal and terrestrial features (Ciochon, 1993; Krentz, 1993a,b; Jablonski et al., 2002, 2008). In total, the available evidence suggests that *T. brumpti* was a terrestrial quadruped that possessed features in the forelimb indicating it was also more arboreal than modern *Theropithecus* and *Papio*, a locomotor repertoire perhaps most similar to that of the modern papionin genus *Mandrillus* (Ciochon, 1993; Krentz, 1993a,b; Jablonski et al., 2002, 2008). The *T. brumpti* forelimb was further specialized for manual foraging, sharing derived characters such as an elongated pollex and shortened second digit with modern geladas (*Theropithecus gelada*) (Jablonski, 1986; Krentz, 1993a,b; Jablonski et al., 2002). Also similar to modern geladas, the *T. brumpti* hindlimb is described as exhibiting features associated with a distinctive squatting and shuffling food-gathering behavior

* Corresponding author.
E-mail address: cgilbert@hunter.cuny.edu (C.C. Gilbert).

0047-2484/$ – see front matter © 2011 Elsevier Ltd. All rights reserved.
doi:10.1016/j.jhevol.2011.04.007

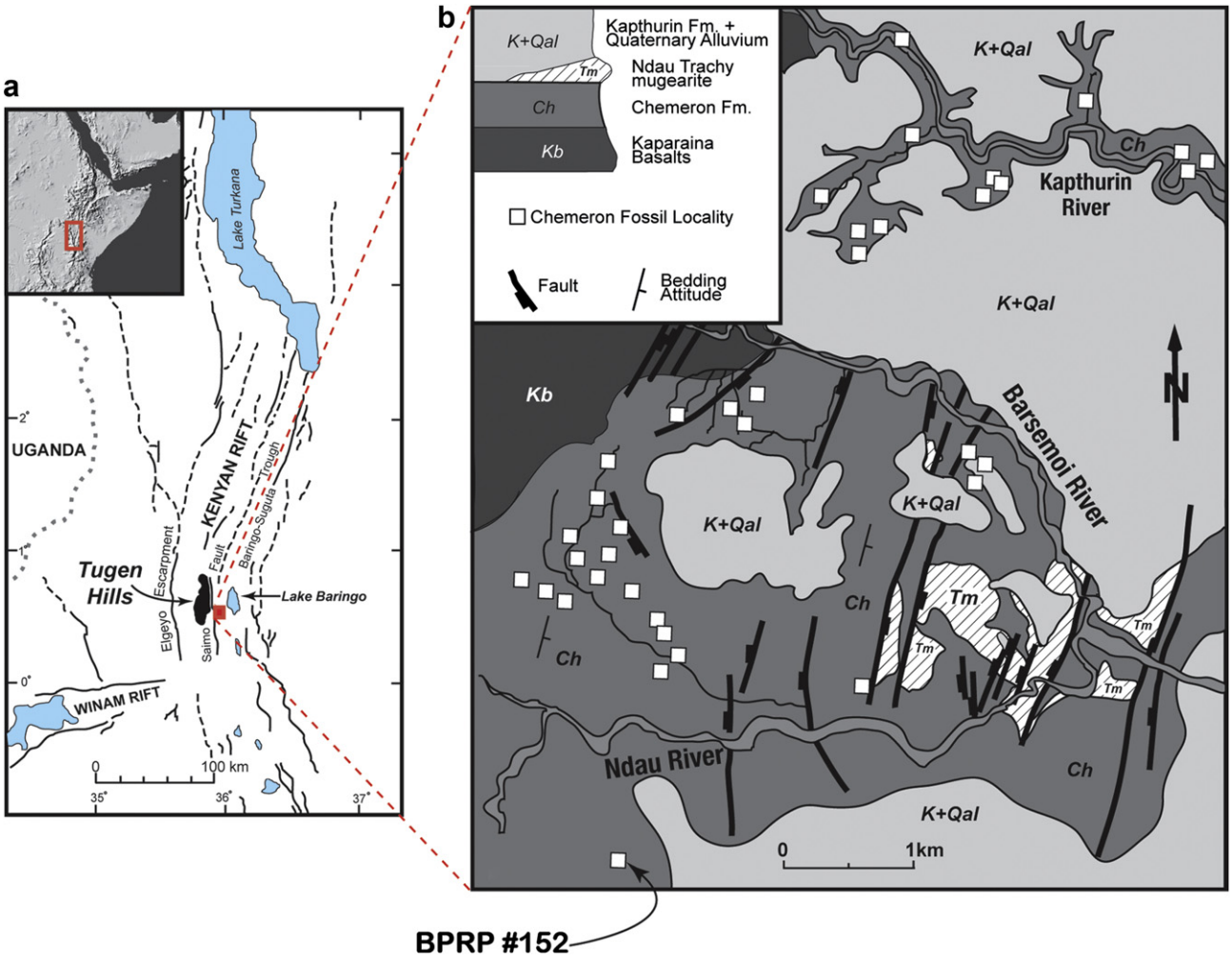

Figure 1. (a) Location of the Tugen Hills and Lake Baringo within the Kenyan Rift Valley. (b) Geologic map of the Chemeron Formation exposed in the Barsemoi, Ndau, and Kapthurin Rivers and associated drainages. Depicted are locations of vertebrate fossil localities including the location of BPRP #152 where the *Theropithecus* partial skeleton was found.

(Krentz, 1993a). Such features of the hindlimb include a "reverse" carrying angle of the femoral shaft and an angulated medial malleolus of the tibia (Krentz, 1993a).

Recently, a partial skeleton of a *T. brumpti* adult male was described from sediments dating to ~3.3 Ma at the site of Lomekwi, West Turkana, Kenya, detailing many aspects of male *T. brumpti* morphology (Jablonski et al., 2002). Thus, from previous research on abundant craniodental and unassociated postcranial remains (e.g., Eck and Jablonski, 1987; Ciochon, 1993; Krentz, 1993a,b), as well as the more recent description of the associated skeleton, the morphology of males is relatively well-known. In contrast, fewer complete cranial and postcranial remains represent the female morphotype. Because of their large size, *T. brumpti* males have been suggested by some to be unlikely arborealists (Jablonski et al., 2002, 2008), but by others to have been more arboreal than modern geladas or *Theropithecus oswaldi* (Krentz, 1993a). Given the large amount of sexual dimorphism and large differences in estimated body mass between *T. brumpti* male and female specimens (males ~36 kg, females ~24 kg; see Delson et al., 2000), it is possible that males and females exhibited slightly different frequencies of arboreal locomotor activities. However, such differences between *T. brumpti* males and females remain to be demonstrated.

Here, we describe a partial skeleton of an aged *T. brumpti* adult female recovered from BPRP site #152 in the Chemeron Formation of the Tugen Hills, Kenya. The associated partial skeleton allows us to address some of the issues relating to the degree of arboreality or terrestriality exhibited by *T. brumpti*, the number of derived features shared with modern geladas, as well as any perceived differences between male and female postcranial morphology and how this affects locomotor reconstruction for this species. In addition, the new specimen allows us to comment on variation within the species and morphological variation in females in particular. While the current analysis is not intended to serve as a comprehensive comparative study of papionin postcranial morphology and levels of variation, the description of KNM-TH 46700 allows us to make some preliminary observations with regards to these issues.

Geological context and associated fauna

Fossiliferous sediments exposed west of Lake Baringo (Fig. 1a) in the Kenyan Rift Valley comprise the most chronologically extensive Neogene clastic sequence known in East Africa, spanning the last 16 m.yr. (Fig. 2) (Hill, 2002). Within this succession, the Chemeron Formation encompasses a series of discontinuous sediments and tuffs exposed over 40 km along the eastern foothills of the Tugen Hills. Chemeron deposits span over 3.7 m.yr. from about 5.3 Ma at the base to less than 1.6 Ma at the top (Fig. 2) (Deino and Hill, 2002; Deino et al., 2002).

In the southernmost exposures of the Chemeron Formation, where BPRP #152 is situated (Fig. 1b), sediments are exposed as an

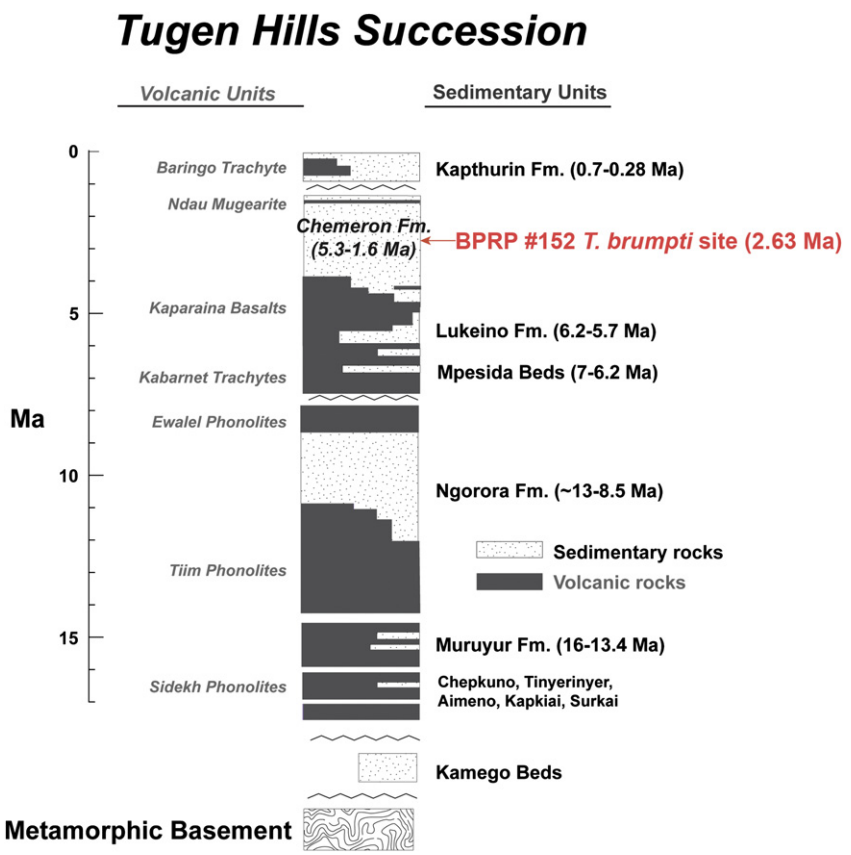

Figure 2. Generalized composite stratigraphic framework of the Tugen Hills Succession, indicating the stratigraphic level of BPRP #152 in the Chemeron Formation.

eastward-dipping structural block (~20–30°) and consist of terrigenous and lacustrine sediments, primarily mudstone, siltstone, and sandstone with intercalations of tuff, diatomite, and conglomerate. Within this general succession, a distinctive lithologic package characterized by a series of diatomite units and interbedded fluvial and alluvial fan detritus and tuffs can be traced >10 km N–S along strike. These sediments document significant, intermittent lake systems within the axial portion of the rift that have been linked directly to precessional cycling (Deino et al., 2006; Kingston et al., 2007). Fossiliferous strata exposed at BPRP #152 are part of this lithostratigraphic package, for which a detailed chronostratigraphic framework has been established (Fig. 3) (Deino et al., 2006). The *T. brumpti* partial skeleton was found in 2003 in lake margin deposits, ~18 m stratigraphically below a tuff dated at 2.59 Ma (Fig. 3).[1] Based on a sedimentation rate of approximately 43 cm/k.yr. calculated for this part of the sequence (Deino et al., 2006), the *T. brumpti* skeleton can be dated to 2.63 Ma.

A list of taxa established from fossils at the *T. brumpti* skeleton site is provided in Table 1. It is not a particularly diverse assemblage, and there are not many specimens, though relatively small sample size probably does not account for the unusual absence of hippopotamids, which are generally ubiquitous at Chemeron sites. In addition, the collection includes specimens belonging to quite rare taxa such as *Panthera* and Neotragini. It is also unusual within the Tugen Hills in having the suid *Metridiochoerus andrewsi* as part of it. This is a relatively common pig in other east African regions over the time range represented by the Chemeron Formation, but the four individuals at BPRP #152 are the only fossils of *M. andrewsi* so far known from the many sites in the entire Chemeron succession (Bishop et al., 1999). The reason for the almost total absence of *M. andrewsi* in the Chemeron, and for its so far exclusive presence at this particular site, is not yet understood. Stable carbon isotope analyses of enamel from chronologically younger *M. andrewsi* teeth suggest an almost exclusive C_4 grass diet (Bishop et al., 1999; Harris and Cerling, 2002), and the relative hypsodonty of these later specimens also supports this notion of obligate grazing. But these earlier Chemeron examples appear to be less hypsodont, and their isotopic, and thus dietary, status is as yet undetermined.

Site BPRP #152 is just one of many fossil localities in this area and time that provide evidence of the local fauna during a period of considerable long-term climatic and environmental fluctuation. Although carbon isotopic analyses of fossil mammalian herbivore enamel and paleosol carbonates from the upper Chemeron Formation (3-2 Ma) (Kingston, 1999) indicate heterogeneous environments with C_3 and C_4 vegetation, it remains unclear how this heterogeneity was partitioned temporally and spatially. In other words, was this portion of the Rift Valley characterized by persistent grassy woodland ecosystems, or were C_3- and C_4-dominated habitats alternating through time? The periodic existence of major astronomically forced lakes in the Rift Valley over the interval from 2.7 Ma to 2.55 Ma, possibly extending across the entire width of the rift (Deino et al., 2006; Kingston et al., 2007; Goble et al., 2008), suggests that ecosystems were oscillating in response to these cyclical changes in precipitation.

[1] The *T. brumpti* specimen was discovered by Julius Kleria, Bonface Kimeu, and JK in the course of geological and paleontological survey work. Local excavation of the areas the skeleton had come from was carried out immediately, and a number of visits to the site were made by them and by AH and EDG in subsequent field seasons to collect additional fauna and other data.

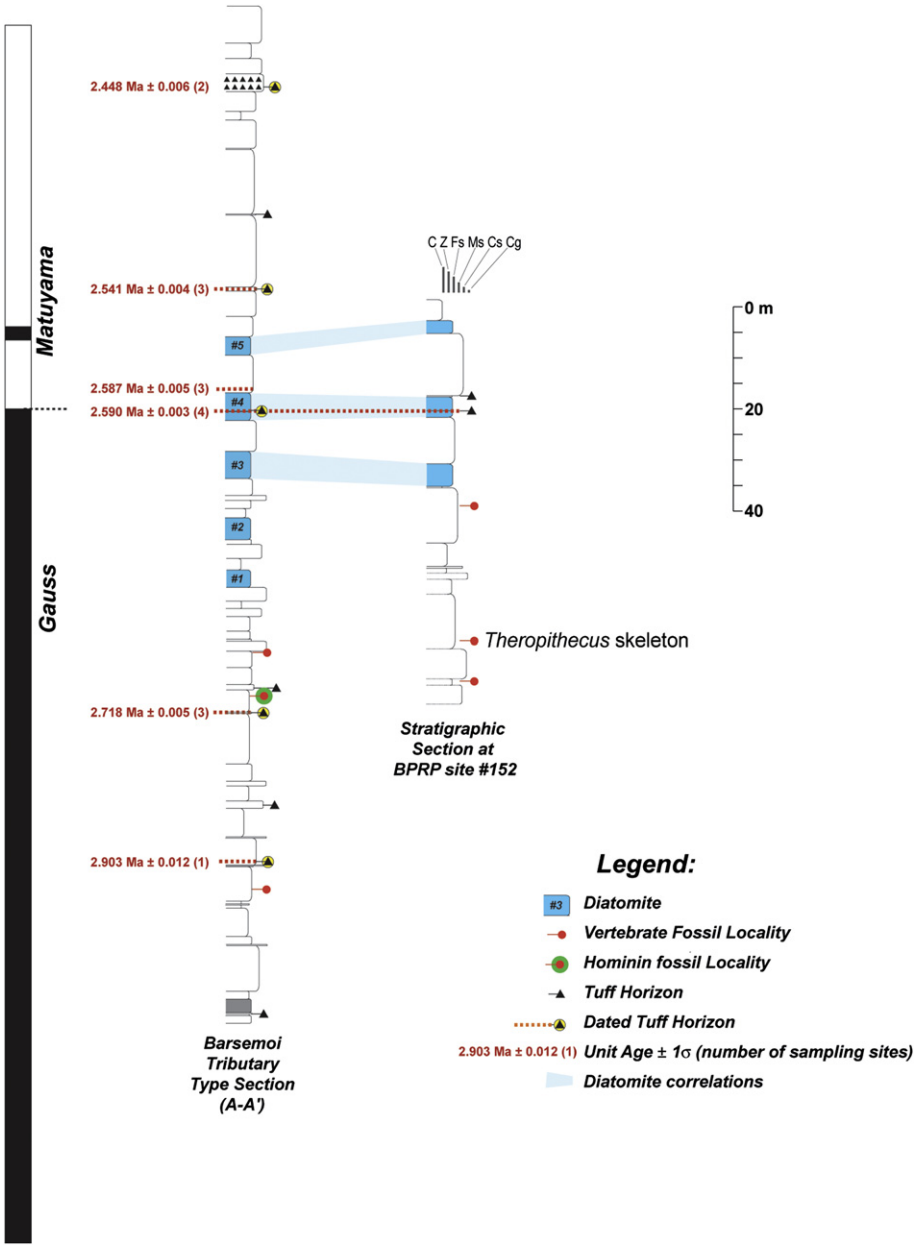

Figure 3. Type stratigraphic section of the Chemeron Formation locally between ca. 3.0 Ma and 2.4 Ma correlated with the section at BPRP #152. Abbreviations are as follows: C = clay, Z = silt, Fs = fine sand, Ms = medium sand, Cs = course sand, and Cg = conglomerate.

Materials and methods

Numerous elements comprise KNM-TH 46700 (Fig. 4; Table 2). The specimen is housed in the National Museums of Kenya, Nairobi. Where available, measurements were taken using digital calipers and recorded to the nearest tenth of a millimeter. Comparative specimens were examined at the both the National Museums of Kenya, Nairobi, and the American Museum of Natural History (AMNH), New York.

Systematic paleontology

Order Primates Linnaeus, 1758
Suborder Anthropoidea Mivart, 1864
Infraorder Catarrhini E. Geoffroy, 1812
Superfamily Cercopithecoidea Gray, 1821
Family Cercopithecidae Gray, 1821
Subfamily Cercopithecinae Gray, 1821
Tribe Papionini Burnett, 1828
Genus *Theropithecus* I. Geoffroy Saint-Hilaire, 1843

(= or including: *Macacus* Rüppell, 1835, in part; *Gelada* Gray, 1843; *Simopithecus* Andrews, 1916; *Theropythecus* Vram, 1922 [*lapsus*?]; *Papio* Erxleben, 1777; Broom and Jensen, 1946, in part; Buettner-Janusch, 1966, in part; *Dinopithecus* Broom, 1937; Arambourg, 1947, in part; Broom and Hughes, 1949, in part; *Brachygnathopithecus* Broom and Robinson, 1949; Kitching, 1952, in part; *T.* [*Omopithecus*] Delson, 1993).

Type species

T. gelada Rüppell, 1835.

Table 1
Faunal list for BPRP #152, Chemeron Formation.

DIPLOPODA			
	Indet.		49698
PISCES			
	Indet.		49704
REPTILIA			
Testudines			
	Testudinidae		
		Geochelone?	49694
	Trionychidae		49692
Crocodilia			
	Crocodylidae		49696, 49699
			49700
MAMMALIA			
Proboscidea			
	Elephantidae		
		Elephas recki	94-237
Primates			
Cercopithecoidea			
	Cercopithecidae		
		Theropithecus brumpti	46700
Carnivora			
	Felidae		
		Panthera sp.	48299
Perissodactyla			
	Equidae		
		"*Hipparion*" sp.	30986, 30987
Artiodactyla			
	Bovidae		
	Bovinae		
	Tragelaphini		48429
	Bovini		
		Simatherium sp.	49712
	Antilopinae		
	Neotragini		49702
	Reduncinae		
	Reduncini		49691
	Hippotraginae		
	Alcelaphini		37213
	Suidae		
		Metridiochoerus andrewsi	32832, 37449

Taxonomic names are followed by the National Museums of Kenya accession numbers (except for *Elephas recki*, which is a BPRP expedition field number), which indicate examples of specimens that we believe establish that taxon at the site. Accession numbers should be prefixed with "KNM-TH". Identifications by EDG and AH.

Other included species

T. oswaldi Andrews, 1916; *T. brumpti* Arambourg, 1947; *T. baringensis* Leakey, 1969.

Generic diagnosis

This diagnosis follows Jolly (1972), Szalay and Delson (1979), Eck and Jablonski (1987), Delson (1993), Jablonski (1993a,b, 2002), and Frost and Delson (2002) with additional observations. *Theropithecus* is a large- to very large-sized papionin with a body mass typically ranging from about 12 kg (females) to 19 kg (males) for the extant *T. gelada*, and an estimated 17–37 kg (females) to 25–89 kg (males) among extinct species (Smith and Jungers, 1997; Delson et al., 2000). The neurocranium is distinguished from that of other papionins by the well-developed and anteriorly placed sagittal crest. The temporal lines usually meet to form the sagittal crest anterior to bregma, and the crest is particularly pronounced in males. In other papionins where sagittal crests are present, the temporal lines usually meet at or posterior to bregma. The supraorbital torus and glabella are, in general, thick and prominent. There is great post-orbital constriction in the *Theropithecus* cranium, and a post-orbital sulcus is typically present.

In dorsal view, differences in papionin anterior temporal line morphology have recently been documented (McGraw and Fleagle, 2006; Gilbert, 2007). In *Mandrillus* and *Cercocebus*, the anterior temporal lines converge posteriorly from the lateral margin of the supraorbital torus, giving the anterior portion of the skull a "visor-like" appearance. In contrast, *Papio* and *Lophocebus* have anterior temporal lines that typically converge medially along the margin of the supraorbital torus and then take a sharp turn posteriorly, giving the anterior portion of the skull a "pinched-in" appearance. *Macaca*, *Dinopithecus*, *Parapapio*, and *Pliopapio* also often have "pinched-in" anterior temporal lines. *Theropithecus* displays a unique anterior temporal line morphology that is also pinched, but in a more gradual way than in *Papio* and *Lophocebus*. The temporal lines in *Theropithecus* generally extend medially from the lateral margin of the supraorbital torus and curve posteriorly in a smooth rather than sharp way around the area of post-orbital constriction (however, see subgeneric diagnosis below). In addition, as mentioned above, the temporal lines of *Theropithecus* quickly converge in the midline and typically meet anterior to bregma to form a sagittal crest.

The zygomatic region of *Theropithecus* is typically broad with the root of the zygomatic arch arising from a wide area of the face. There is a steep anteorbital drop in the lateral facial profile, and this drop is typically steeper and longer than in other papionins. The face is generally tall, and this height is mostly due to the vertically tall maxillae. The premaxillae are short in comparison to the maxillae, similar only to *Paradolichopithecus* among papionin genera (Frost and Delson, 2002). In all but the largest *Theropithecus* taxa (i.e., *Theropithecus oswaldi oswaldi* and *Theropithecus oswaldi leakeyi*), maxillary fossae are typically present in both males and females.

On the basicranium of *Theropithecus*, two features are of diagnostic interest. On the temporal bone, the postglenoid process is typically taller than that of other papionins, and it is extremely tall in the larger species. On the basioccipital, just anterior to the foramen magnum, there are two well-defined fossae on either side of the midline, most likely associated with internal neck musculature (longus capitis). While other papionins are variable in the development of these fossae, *Theropithecus* almost invariably has well-defined to deeply excavated fossae (see Gilbert, 2008; Gilbert et al., 2009).

The dentition of *Theropithecus* is particularly distinct among papionin genera. The incisors are reduced compared to other papionins (Jolly, 1972); in addition, the incisors are approximately equal in

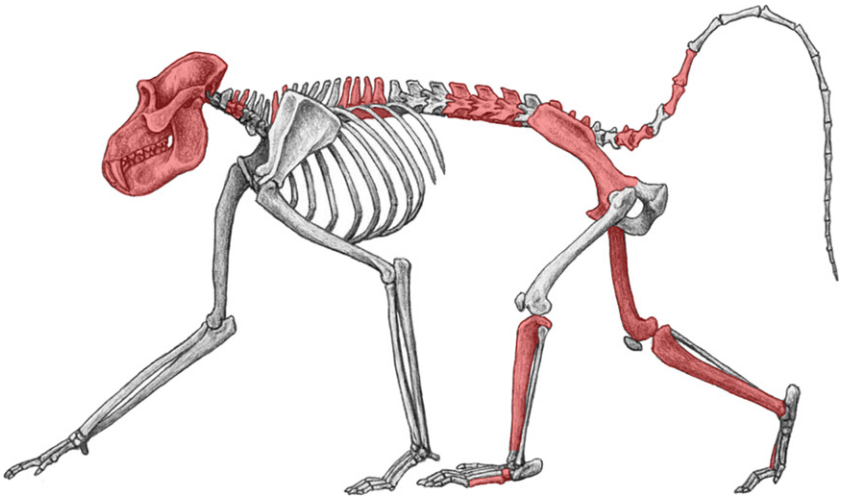

Figure 4. An illustration of a *T. brumpti* male skeleton, courtesy of M. Antón. The shaded elements indicate those present in the female partial skeleton KNM-TH 46700.

size whereas other papionin genera display central incisors that are typically much larger than the lateral incisors. The molars of *Theropithecus* are high crowned and thick-enameled with deep foveae and greatly increased cuspal relief (Jolly, 1972). The cusps are tall and columnar and the increased relief creates deep notches between them. Often, accessory cuspules are found in these intercuspal notches. In addition, the lower molars often display mesiolingually angled lophids and sometimes a large distal accessory cuspule on M_{1-2} (Frost and Delson, 2002). A reversed Curve of Spee gives the entire mandibular row an antero-posterior convexity most obviously seen in lateral view, and the posterior molars have a delayed eruption pattern compared to that seen in other papionin monkeys (Jablonski, 1994). The infoldings of enamel on the molars result in a unique wear pattern (see Szalay and Delson, 1979; Jablonski, 1994).

Table 2
Elements preserved of *T. brumpti* adult female specimen KNM-TH 46700 from BPRP #152.

Element	Brief description
Cranium	Complete but slightly crushed cranium preserving everything except for the upper incisors, upper canines, and right zygomatic arch
Mandible	Mandible in 3 pieces, preserving both corpora, the symphysis, the left ascending ramus, and portions of the dentition from P_3-M_3. Lower incisors, canines, and right ascending ramus are not preserved.
Cervical vertebra	Cervical vertebra (C3–C6)
Cervical vertebra	Portion of cervical vertebra (C3–C6)
Thoracic vertebra	Spinous process of an upper thoracic vertebra
Thoracic vertebra	Spinous and transverse process of an upper thoracic vertebra
Thoracic vertebra	Body of a lower thoracic vertebra
Thoracic vertebra	Body of a lower thoracic vertebra
Thoracic vertebra	Body of a lower thoracic vertebra
Thoracic vertebra	Body of a lower thoracic vertebra
Ribs	Rib fragment
Lumbar vertebra	Lumbar vertebra (L3–L6)
Lumbar vertebra	Lumbar vertebra (L3–L6)
Lumbar vertebra	Lumbar vertebra (L3–L6)
Sacral vertebrae	Sacrum (fused Cd1–Cd3)
Caudal vertebra	Caudal vertebra (Cd6?)
Caudal vertebra	Caudal vertebra (Cd7?)
Caudal vertebra	Caudal vertebra (Cd9?)
Caudal vertebra	Caudal vertebra (Cd10?)
Caudal vertebra	Portion of caudal vertebra
Caudal vertebra	Portion of caudal vertebra
Caudal vertebra	Portion of caudal vertebra
Caudal vertebra	Portion of caudal vertebra
Pelvis	Partial pelvis preserving most of the left ilium, part of the left pubis, and part of the left ischium
Femur	Complete right femur
Tibia	Complete right tibia
Tibia	Partial left tibia preserving the proximal end and most of the shaft
Cuboid	Left cuboid
Metatarsal	Proximal portion of left metatarsal V
Metatarsal	Proximal portion of right metatarsal III

The mandible of *Theropithecus* is generally characterized by a relatively deep corpus and typically displays a more upright or vertical ramus than other large papionin taxa (Jolly, 1972). The symphysis is typically robust and, as is the case with other large papionins, mental ridges are present in males and sometimes females. Similar to the situation with the facial fossae, mandibular corpus fossae are typically found in all but the largest *Theropithecus* taxa.

Postcranially, the extant *T. gelada* is diagnosed by several characters, only a few of which are documented in the fossil taxa and can therefore be attributed to the genus. *Theropithecus* displays unique proportions in the hand bones where the first metacarpals are elongated and the second metacarpals are shortened. The result is an elongated pollex and a shortened second digit, which leads to *Theropithecus* possessing a high opposability index (Napier and Napier, 1967; Jablonski, 1986). The manual and pedal phalanges are short relative to their breadth as well as to overall hand and foot length (Jolly, 1972; Strasser, 1992; Frost and Delson, 2002). The ulnar olecranon process is retroflexed and extends dorsally, similar to the condition observed in other highly terrestrial monkeys. The femur displays a reversed carrying angle, which Krentz (1993a) suggested is related to habitual sitting and the unique "bottom shuffling" form of locomotion found in the extant members of the genus.

Theropithecus (*Omopithecus*) Delson, 1993

(= or including: *Dinopithecus* Broom, 1937; Arambourg, 1947, in part; *Simopithecus* Andrews, 1916; Freedman, 1957, in part. New and unnamed subgenus: Szalay and Delson, 1979).

Type species

T. brumpti Arambourg, 1947

Subgeneric diagnosis

Following the diagnosis of Delson (1993), along with observations by Eck and Jablonski (1984, 1987) and Jablonski et al. (2008),

Theropithecus (*Omopithecus*) is distinguished from *Theropithecus* (*Theropithecus*) facially by a relatively elongated, *Papio*-like, flattened, muzzle dorsum with well-developed maxillary ridges and moderate to well-developed maxillary fossae. The zygomata are anteriorly expanded, with a very robust zygomatic arch that is triangular in cross-section. The anteriormost portion of the zygomatic arch is highly distinctive with a supero-lateral "twisting" on the inferior portion of its base, a feature which is most obviously exaggerated in males. In dorsal view, the neurocranium of some *T.* (*Omopithecus*), particularly males, displays sharply pinched-in temporal lines, a morphology which is not seen in *T.* (*Theropithecus*). This pinched-in morphology appears to be variable in *T. (Omopithecus*). The mandible of *T.* (*Omopithecus*) is characterized by a robust mandibular symphysis with sinusoidal mental ridges and a rugose mental protuberance.

Postcranially, *T.* (*Omopithecus*) exhibits adaptations for elbow stability but also shoulder flexibility, as demonstrated by Jablonski (1993a), Jablonski et al. (2002), and Krentz (1993a). The humerus is characterized by tuberosities that are subequal in size and lie inferior to the level of the humeral head. The intertubercular groove on the proximal humerus is shallow. The proximal ulna displays a robust, retroflexed, and moderately elevated olecranon process as well as a superomedially projecting bony olecranon prominence in ventral view.

Note that we tentatively exclude *T baringensis* from the *T.* (*Omopithecus*) subgenus until further evidence demonstrates its phylogenetic position securely in the *T. brumpti* clade rather than a basal member of the genus (e.g., see Gilbert, 2008, 2009).

Theropithecus (*Omopithecus*) *brumpti* Arambourg, 1947

Lectotype

MNHN-P Omo 001, a left maxillary fragment preserving M^2 and an unerupted M^3 (selected by Eck and Howell, 1982).

Specific diagnosis

As for subgenus.

Referred material

KNM-TH 46700.

Horizon

Chemeron Formation outcrops, Tugen Hills, Kenya.

Localities/sites

Chemeron Formation BPRP #152, 2.63 Ma.

Description

Cranium The cranium is nearly complete, save for the upper incisors, upper canines, and the right zygomatic arch (Fig. 5). The entire cranium has been dorsoventrally flattened during fossilization, so that the orbits are distorted and the cranium appears anteroposteriorly longer than it should in dorsal view. From the inferior orbital margin downward, there appears to be much less distortion in terms of dorsoventral flattening; however, the maxillary fossa on the right side of the muzzle appears deeper and more distinct than the left side due to another distortion during fossilization. The nasal bones and the nasal aperture are both distorted laterally to the right, suggesting some crushing and/or distortion originating from the left side of the face.

In frontal view, glabella and the supraorbital region are prominent. A post-orbital sulcus is present. Superiorly, the frontal processes of the maxilla meet in the midline and, consequently, there is no projection of the nasal bones above the maxillofrontal suture. The orbits are crushed vertically with the lateral orbital

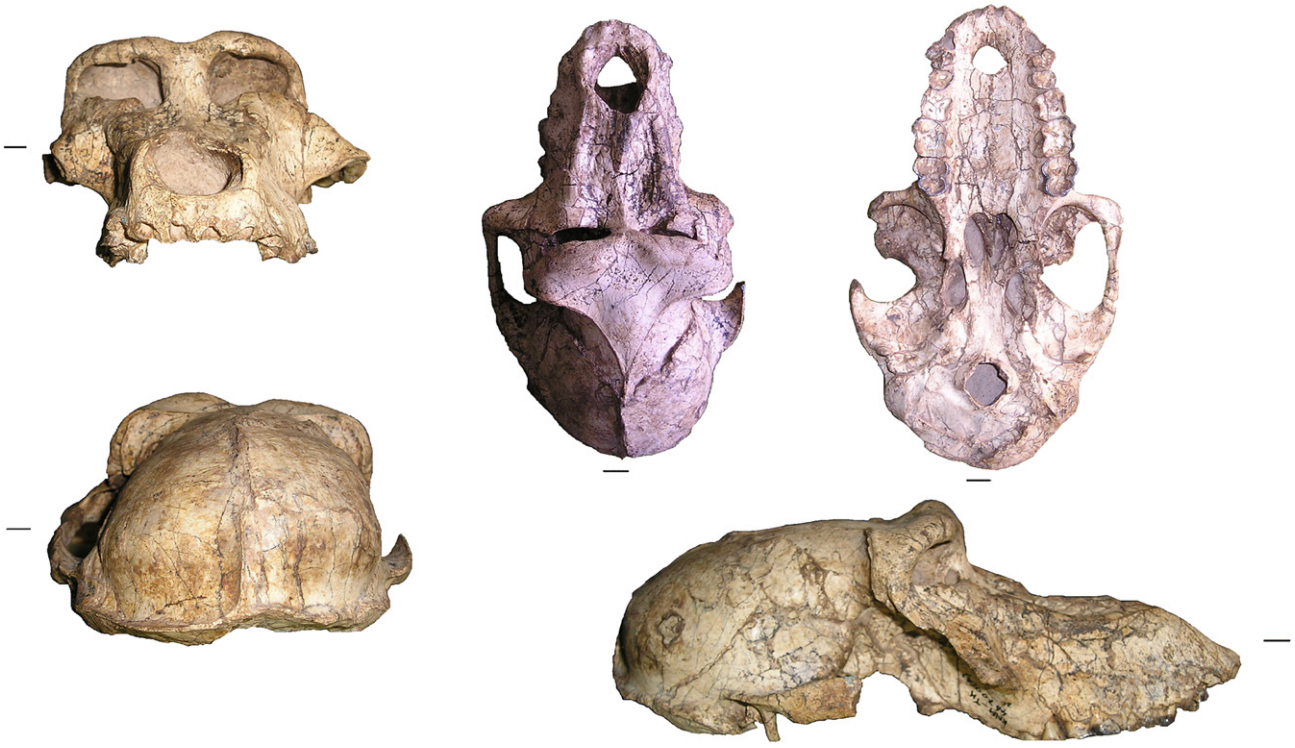

Figure 5. The cranium of KNM-TH 46700. Clockwise from upper left: anterior view; dorsal view; basicranial view; lateral view; posterior view. Scale = 1 cm.

margins having broken inwards and posteriorly, giving the orbits a very rectangular outline (Fig. 5).

The muzzle dorsum appears flat and the nasals are not raised relative to the dorsum. Laterally, the muzzle is dominated by prominent maxillary ridges that extend from the inferior orbital margin to the nasal aperture. On the side of the muzzle, maxillary fossae extend up to the infraorbital plate. The nasal bones are distorted to the right distally and the nasal aperture appears large and is distorted to the right.

In dorsal view, the cranium displays the typical and distinctive *Theropithecus* temporal line pattern. The temporal lines are pinched, but follow the outline of the anterior portion of the calvaria and the area of post-orbital constriction quite closely. The temporal lines converge quickly as they move posteriorly, meeting approximately 6 mm anterior to bregma. Even though this is a female specimen, a sagittal crest is formed as the temporal lines converge and move posteriorly, and a well-formed, laterally-extended nuchal crest meets the sagittal crest at inion. As the development of the temporal lines has been noted to be an age-related feature (Jolly, 1972), the sagittal crest development observed in this specimen is most likely attributable to its advanced age. Around inion, the nuchal crest is upturned on the right side, but this appears due to distortion. The left side shows no evidence of upturn or downturn, making it most likely that the nuchal crest was relatively straight prior to distortion during fossilization.

Laterally, the left zygomatic is intact while the right zygomatic is broken. The zygomatic arch is much more gracile than in *T. brumpti* males, but the maxillo-zygomatic portion (i.e., the infraorbital plate) extends laterally, beginning at the level of the distal loph of the M^3, and the anteriormost portion of the arch hints at the male morphology with a supero-lateral "twisting" of the inferior portion at the beginning of the arch. The zygomatic arch is well-built (moderate to heavy for a female papionin) but, again, not nearly as massive as in *T. brumpti* males, and not as heavily built as in the subadult female NME L32-155 or the adult female NME L122-34 from the Omo Shungura Formation, both of which are younger females than KNM-TH 46700. An adult female from the Turkana Basin at Koobi Fora, KNM-ER 4704, has also recently been described as possessing more weakly flaring zygomatic arches compared to other *T. brumpti* specimens (Jablonski et al., 2008). Given the amount of variation seen in the build of the male zygomatic region (e.g., see Eck and Jablonski, 1987; Jablonski, 1993b; Leakey, 1993), the level of variation that KNM-TH 46700 and the Koobi Fora specimen introduce into the female population seems acceptable.

The basicranium of KNM-TH 46700 appears relatively unflexed, but some portion of this is probably due to the dorsoventral flattening of the skull. The external auditory meatus (EAM) extends laterally and posteriorly and ends at a point posterior to basion and medial to the lateral margin of the skull (i.e., EAM is overhung by a suprameatal roof). The EAM is slightly separated from the post-glenoid process, which is quite tall but not nearly as tall as seen in *T. o. oswaldi* and *T. o. leakeyi* specimens. Fossae are definitely present anterior to the foramen magnum, but they are not as well excavated as typically seen in many *T. brumpti* and *T. gelada* specimens. The inferior petrous processes are slightly distorted in appearance, with the left side appearing more laterally positioned than the right side. The choanae are slightly distorted, but appear widely divergent as they proceed anteriorly.

The preserved dental elements are extremely worn, suggesting that this was an elderly female at the time of death. It is also possible that the extreme dental wear is indicative of a particularly harsh diet, but additional microwear analyses will be necessary to more precisely infer the dietary regime of this specimen. The right and left P^3-M^3 are preserved, but due to extreme wear, no obvious morphological features can be discerned. The incisors and canines are not

Table 3
Selected craniodental measurements of *T. brumpti* adult female specimen KNM-TH 46700 in mm.

Specimen	Element	Gl-In	Br-Ba	Min Frontal Breadth	Po-Po	Gl-Br	La-In	Op-In	Op-Ba	Eur-Eur	Car-Car	Ba-Spb	Po-Pr	Na-Pr	Na-Rh	Zy-Zy	Po-Gl	Max Biorbital Breadth
KNM-TH 47670	Cranium	116.0	55.0	52.0	76.0	68.0	(11.0)	38.0	17.0	80.0	30.0	19.0	153.0	94.0	49.0	(110.0)	88.0	85.0
		Ect-Ect	Palate Length	Min Malar Height	Zym-Zym	P^3 MD	P^3 BL	P^4 MD	P^4 BL	M^1 MD	M^1 MBL	M^1 DBL	M^2 MD	M^2 MBL	M^2 DBL	M^3 MD	M^3 MBL	M^3 DBL
	Palate and Upper Dentition	58.0	77.0	33.0	(84.0)	(6.8)	(9.4)	(7.8)	(9.8)	(11.2)	(11.3)	(11.0)	14.9	13.4	12.3	15.2	13.9	12.0
		Max Sym Height	Max Sym Depth	Corpus Height at M_1	Corpus Width at M_1	Corpus Height at M_3	Corpus Width at M_3	P_3MD	P_3 BL	P_4MD	P_4 BL	M_1 MD	M_2 MD	M_2 MBL	M_2 DBL	M_3 MD	M_3 MBL	M_3 DBL
	Mandible and Lower Dentition	(40.0)	(20.0)	35.0	15.0	36.0	16.0	(7.8)	(5.8)	(9.0)	(7.4)	X	(14.7)	11.7	11.8	(19.1)	13.1	11.8

Notes: Gl = glabella, In = inion, Br = bregma, Ba = basion, Po = porion, La = lambda, Op = opisthion, Eur = euryon, Car = carotid canal, Spb = sphenobasion, Pr = prosthion, Na = nasion, Rh = rhinion, Zy = zygion, Ect = ectomolare, Zym = zygomaxillare, Min Malar Height = distance from inferior orbital margin to the inferior border of the zygomatic process of the maxillas, MD = mesiodistal length, BL = buccolingual breadth, MBL = mesial buccolingual breadth, DBL = distal buccolingual breadth, Sym = symphyseal. X = measurement unavailable. Numbers in parentheses represent estimates. Note that P_3MD refers to occlusal length only and does not include the length of the honing flange. When available, dental measurements represent averages of the left and right sides.

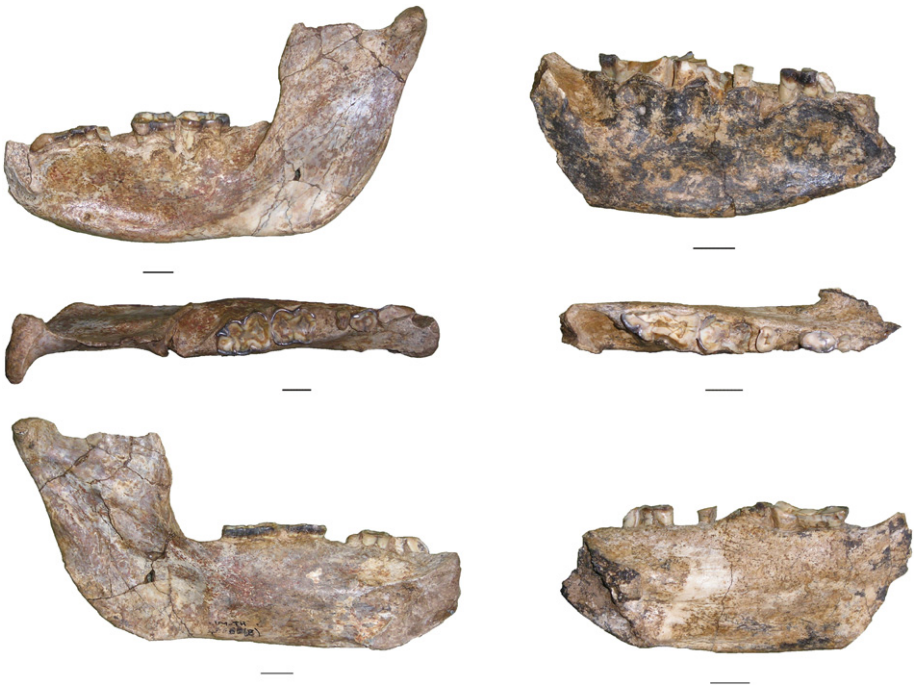

Figure 6. The mandible of KNM-TH 46700. Top left: left lateral view. Middle left: occlusal left view. Bottom left: medial left view. Top right: right lateral view. Middle right: occlusal right view. Bottom right: medial right view. Scale = 1 cm.

preserved in the maxilla, but their alveoli are present. The small size of the incisor alveoli suggest that the incisors would have been relatively small, as is typical of *Theropithecus* taxa. An isolated and extremely worn upper left canine was also found with the skeleton. Available cranial and dental measurements are provided in Table 3.

Mandible The mandible is preserved in three pieces (Fig. 6). Both halves of the mandible are preserved, from the midline of the symphysis and including both corpora and the entire left ascending ramus. The left condyle is preserved, but the left coronoid process is not. Only a portion of the right ramus is preserved. P_3-M_3 are preserved on the left half of the mandible, but what remains of the left M_1 is heavily damaged and most of this tooth has fallen out of its socket (Fig. 6). The left incisors and canines are not preserved in the mandible. On the right half of the mandible, P_3 is heavily damaged (only the posterior portion remains and the rest of the tooth is broken), P_4 is mostly intact, M_1 is heavily damaged (only the posterior portion remains), M_2 is heavily damaged (a large portion of the mesial half of the tooth is missing, but the distal lophid remains), and M_3 is heavily worn and heavily damaged. On the mandibular corpus, a well-developed mandibular corpus fossa is present. On the left side, the ascending ramus is very tall and moderately posteriorly inclined. There is no expansion of the gonial region at the base of the ramus.

The lower dentition is also extremely worn and there are no visible morphological features on the individual teeth due to the extreme wear. The extramolar sulcus appears relatively wide for a cercopithecine, but it is possible that the advanced ontogenetic age of the specimen has contributed to this appearance. On the mandibular symphysis, prominent mental ridges are present, but a median mental foramen cannot be discerned. The lack of a median mental foramen may simply be due to poor preservation (the mandible is broken into three pieces), as median mental foramina are typical in *Theropithecus* species. In occlusal view, the inferior portion of the mandibular symphysis extends posteriorly to approximately the level of the P_4. In addition to the worn dental remains preserved in the mandible, an additional isolated tooth (probably a lower canine) was also found but could not be positively identified to serial position.

Axial skeleton The axial skeleton is represented by portions of 2 cervical vertebrae, 6 thoracic vertebrae, 1 large rib fragment, 3 lumbar vertebrae, the sacrum, and 8 caudal vertebrae. There is one additional piece of bone that appears to be a portion of a vertebra, but this fragment cannot be confidently identified. A fairly complete cervical vertebra, most likely somewhere in the C3–C6 region based on the short and robust spinous process, is present with a small section of another cervical vertebra fused distally on the left side. The cranial zygapophyses are oriented craniodorsally and transverse foramina are present at the base of the transverse processes, just ventral to the zygapophyses. The right transverse process is completely broken off, but a portion of the left transverse process is present and oriented ventrolaterally. The right caudal zygapophysis is visible and is oriented caudoventrally.

Moving caudally, dorsal portions of two upper thoracic vertebrae are present; one preserves the spinous process, the left transverse process with a rib facet, and a small portion of the left caudal zygapophysis oriented ventromedially; the other preserves the

Table 4
Selected vertebral measurements of *T. brumpti* adult female specimen KNM-TH 46700 in mm.

Vertebral element	Max cranial-caudal vertebral body length
Lower thoracic vertebra	12.9
Lower thoracic vertebra	13.5
Lower thoracic vertebra	13.6
Lower thoracic vertebra	15.2
L3/L4?	24.9
L4/L5?	29.5
L5/L6?	31.5
Sacrum (fused Cd1–Cd3)	51.8
Cd6?	19.6
Cd7?	25.8
Cd9?	46.5
Cd10?	44.3

spinous process, the transverse processes with rib facets, the superior portion of the vertebral foramen, one cranial zygapophysis oriented dorsolaterally, and both caudal zygapophyses oriented ventromedially. Four lower thoracic vertebrae preserving mostly just the bodies are also present. The bodies are relatively small, especially compared to the lumbar vertebral bodies (see Table 4 for measurements). These are identified as lower thoracic vertebrae due to the presence of rib facets. No spinous or transverse processes are preserved. One rib fragment is present, but cannot be identified to position.

A total of three lumbar vertebrae are present, most likely representing three of the four positions between L3 and L6. Measurements of the maximum cranio-caudal vertebral body length are given in Table 4. The most cranial of the lumbar vertebrae, L3 or L4, possesses cranial zygapophyses that are oriented dorsomedially at approximately 45°, slightly more medial than dorsal. The spinous and transverse processes are broken off just distal to the base of the process, and the transverse processes originate off the dorsal half of the vertebral body. The caudal zygapophyses are oriented ventrolaterally, also at an angle of approximately 45°, and slightly more lateral than ventral.

The L4/L5 vertebra displays cranial zygapophyses that are broken and damaged, but enough of the left cranial zygapophysis remains to infer that it is oriented dorsomedially. The spinous process is preserved and is relatively short and stout, as is typical of lumbar vertebrae. A good portion of the right transverse process is present while only the base of the left transverse process is preserved. The transverse processes originate from the top portion of the vertebral body, higher up dorsally than in L3/L4. The caudal zygapophyses are again oriented ventrolaterally.

The most caudal of the lumbar vertebrae, most likely L5/L6, displays cranial zygapophyses that are still covered in matrix, making it impossible to accurately describe their morphology and position. The spinous process is present and relatively stout and thick. About half of the left transverse process is still present, while the right transverse process is broken off at the base. Again, the transverse processes originate on the dorsal half of the vertebral body. The caudal zygapophyses are oriented ventrolaterally, but more ventral than the more cranial lumbar vertebrae described here.

Finally, a complete sacrum and portions of eight caudal vertebrae are present. S1–S3 are fused and preserved as the sacrum; vertebrae tentatively identified as Cd3, Cd4, Cd6, and Cd7 are also present. The remaining caudal vertebrae are fragmentary and unidentifiable. The maximum length of the sacrum and caudal vertebral bodies are given in Table 4.

Pelvis The left portion of the pelvis preserving most of the ilium, part of the pubis, and part of the ischium is present. The iliac blade appears tall, as is typical of monkeys; however, the superior portion and dorsolateral half of the iliac blade is missing. Most of the pubis is preserved and appears relatively long (preserved length ~71 mm, see Table 5), but not out of the range of other cercopithecine taxa. An outline of the anterior portion of the obturator foramen is visible, but it is impossible to discern its shape because most of the ischium is not preserved. About three-quarters of the acetabulum are preserved, and the ilium is relatively wide compared to the estimated acetabular diameter (see Fig. 7). The presence of a wide ilium is not typically seen in modern *T. gelada* or in the

Figure 7. The partial pelvis of KNM-TH 46700. Scale = 1 cm.

Table 5
Measurements of the pelvis in mm.

Measurement	Taxon (Specimen #)		Taxon (Sample Size)						
	T. brumpti (KNM-TH 46700)	*T. brumpti* (KNM-ER 4704)	*T. oswaldi* (*n* = 2)	*T. gelada* females (*n* = 2)	*Papio* females (*n* = 3)	*Lophocebus* females (*n* = 12)	*Cercocebus* females (*n* = 7)	*Mandrillus* females (*n* = 3)	*Macaca* females (*n* = 13)
Max acetabular diameter	(25.5)	20.4	36.7	X	X	X	X	X	X
Min width of the ilium	30.2	X	36.4	X	X	X	X	X	X
Ilium width / acetabulum breadth x 100	(118.4)	X	99.1	104.1	118.4	95.3	106.0	105.4	108.5
Preserved pubis max length from medial lip of acetabulum	(71.0)	X	X	X	X	X	X	X	X

Notes: X = unavailable measurement. Numbers in parentheses represent estimates. Measurements for adult female *T. brumpti* KNM-ER 4704 taken from Jablonski et al. (2008). *T. oswaldi* specimens include Olduvai MCKII 067/5594 and KNM-ER 866. For the extant papionin taxa, numbers included represent averages taken from Fleagle and McGraw (2002).

T. oswaldi specimen we examined (Table 5), but it is common in modern *Macaca*, *Cercocebus*, and *Mandrillus*, and also seen in *Papio hamadryas* females (Fleagle and McGraw, 2002).

Femur A complete right femur is present that is extremely well-preserved with no apparent distortion (Fig. 8). The overall size of the bone is slightly larger than a *Papio h. cynocephalus* male, and the average body mass for the female *T. brumpti* population as represented by this specimen is ~22.2 kg based on the transverse (ML) diameter of the femoral midshaft (see regression equations in Delson et al. [2000]). The shaft is anteroposteriorly bowed to a very large degree. In fact, the bowing of the shaft is much greater than that seen in *Papio* or *T. gelada* and most similar to the geologically younger *T. oswaldi* subspecies. As it moves distally, the shaft is relatively straight and does not bow laterally. The femoral neck is shorter than observed in *Papio* but typical of *Theropithecus* (Krentz, 1993a). The angle of the neck relative to the head is relatively low, but it is not horizontal. A fovea capitis is present on the femoral head and the fovea appears relatively shallow compared to specimens of *T. oswaldi* and *Papio*, although this phenomenon could be due to weathering. On the superior to posterior surface of the femoral head, the articular surface extends laterally and expands onto the femoral neck (Fig. 8). Similar to the condition described for other *Theropithecus* species, both extinct and extant (see Krentz, 1993a), the greater trochanter rises high above the femoral neck and the relative height of the greater trochanter is great (Table 6); *Theropithecus* species index averages range from 6.0 to 6.4 (see Krentz, 1993a). The greater trochanter is curved proximo-medially (takes a medial excursion), similar to other *Theropithecus* species, but is not as vertical as Krentz (1993a) described for other *T. brumpti* femora. The lesser trochanter is relatively large and posteriorly-to-posteromedially directed (Fig. 8; Table 6).

Distally, the patellar groove is well-defined and appears narrow relative to intercondylar width. The lips of the patellar groove are moderately- to well-developed. The medial lip is relatively rounded and the lateral lip is prominent and slightly taller than the medial lip (Fig. 8). In anterior view, the lateral condyle is larger and more distally extended compared to the medial condyle. Reflecting the origins of the medial and lateral collateral ligaments, there are deep or pronounced depressions on the medial side of the medial condyle and the lateral side of the lateral condyle, respectively. The epicondyles are rounded and not very prominent. In distal view, the intercondylar notch is shallower than seen in *T. oswaldi*, and overall more similar to *Papio* and *T. gelada*. In distal view, and in the antero-posterior dimension, the medial condyle is slightly longer or more posteriorly oriented than the lateral condyle, but less so than seen in *T. oswaldi* and some *Papio* males. In this respect, the distal femur is most similar to the *Papio* females and *T. gelada* femora we examined. In posterior view, the medial condyle is wider than the lateral condyle. Finally, although Krentz (1993a) discussed a distinct reverse carrying angle, or a lateral angling of the shaft distally onto the condyles (defined and figured as character 56 in his Table 14.3 and Fig. 14.8, respectively), of 8–10°, we only notice a slight distolateral excursion in KNM-TH 46700. Following Krentz's (1993a) definition, this specimen lacks a pronounced reverse carrying angle. In fact, the degree of lateral excursion exhibited by KNM-TH 46700 overlaps with the range of variation observed by the authors in both modern *T. gelada* and *P. hamadryas* spp. (Fig. 9).

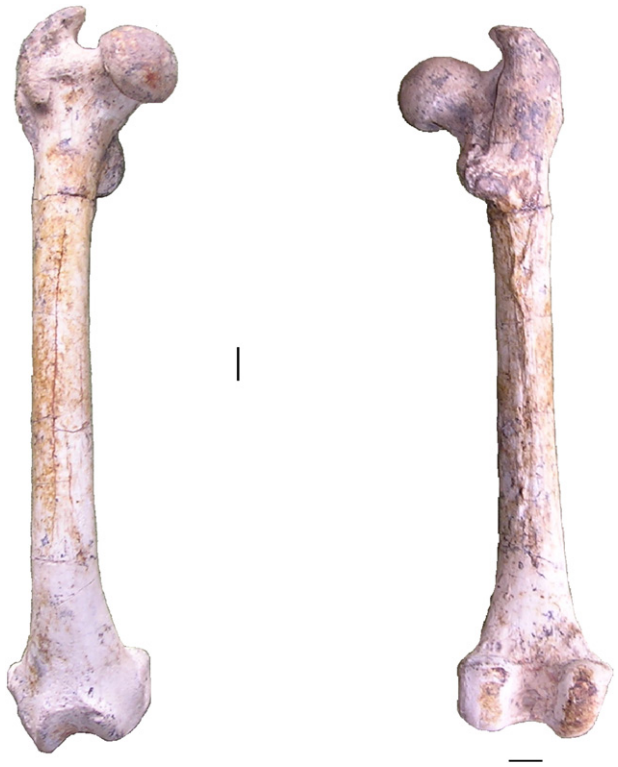

Figure 8. The right femur of KNM-TH 46700 in anterior (left) and posterior (right) views. Scale = 1 cm.

Table 6
Femoral measurements in mm.

Measurement	*T. brumpti* (KNM-TH 46700)
Max length of femur	218.7
SI diameter of femoral head	23.3
ML width of femoral head	20.3
Max diameter of femoral head	24.7
PD distance between highest point on head and lowest point on neck	15.0
PD distance between highest point on greater trochanter and lowest point on neck	13.8
AP diameter of proximal shaft	17.0
ML diameter of proximal shaft	16.9
Bicondylar width	41.5
AP diameter of lateral condyle measured from the lip	34.8
ML width of patellar surface	23.4
PD length of patellar surface	24.5
AP diameter at midshaft	16.9
ML diameter at midshaft	16.3
Relative height of greater trochanter	6.3

Notes: SI = superior–inferior; ML = medial–lateral; PD = proximal–distal; AP = anterior–posterior.

Tibiae The complete right tibia is present and portions of the left tibia, specifically the proximal end along with most of the shaft, are also present. Distally, the medial malleolus does not appear to be angled at 45° as described by Krentz (1993a). Instead, it appears most similar to modern *Papio* and has relatively little angulation in anterior view (Fig. 10). *T. oswaldi* and *T. gelada* appear slightly more angled, but not to the same degree as seen in colobines. The right tibial shaft is bowed anteriorly and laterally to a significant degree. *T. oswaldi* also displays this tibial morphology and, to a lesser extent, so do modern *Papio* and modern *T. gelada*. It is unclear if the mediolateral bowing of the tibial shaft is related to a squatting and shuffling behavior similar to modern geladas. However, the degree of mediolateral bowing in *T. oswaldi* and *T. brumpti* is much greater than that seen in modern *Papio*, *T. gelada*, or *Colobus*.

At the proximal end of the shaft, a prominent tibial tuberosity is present. On the proximal articular surface, the medial condyle is slightly larger than the lateral condyle, reflecting the articulation with the femur, and the medial condyle extends slightly farther

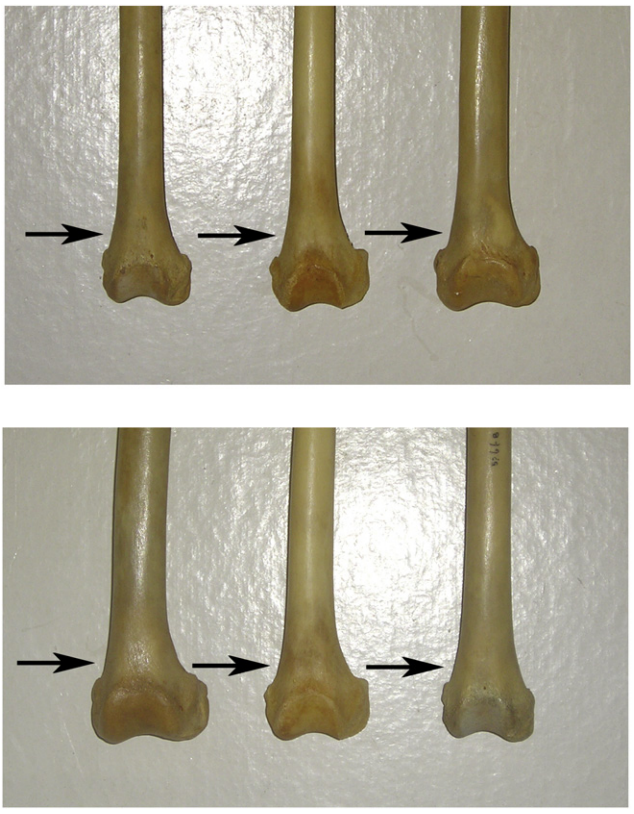

Figure 9. Distal femora in anterior views. Top panel, right femora (reversed for comparison), from left to right: *P. h. anubis* female AMNH 52668, *T. gelada* male AMNH 60568, *P. h. ursinus* male AMNH 80774. Bottom panel, left femora, from left to right: *P. h. ursinus* male AMNH 80774, *T. gelada* male AMNH 60568, *P. h. anubis* female AMNH 52668. Black arrows highlight the "reverse carrying angle," or the lateral angling of the shaft onto the condyles, as described and illustrated in Krentz (1993a: Fig. 14.8). Note the variation and overlap in reverse carrying angles among the specimens. Compare with Fig. 8.

Figure 10. The tibiae of KNM-TH 46700 in anterior view. Left: right tibia. Right: left tibia. Scale = 1 cm.

posteriorly. At the midshaft, the tibia is relatively elongated anteroposteriorly, similar to modern geladas, *Papio*, and *Lophocebus* (Fleagle and McGraw, 2002). The lack of anterior–posterior compression seen in the tibial shaft of KNM-TH 46700 is notable even when compared to living geladas, and this condition appears to be even more exaggerated in another *T. brumpti* specimen, the adult male KNM-WT 39368 (Table 7). However, since the KNM-WT 39368 tibia was crushed and reconstructed, KNM-TH 46700 may represent a more typical morphology. The left tibia of KNM-TH 46700 is similar in size and shape to the complete right tibia, obviating a separate description. Measurements of both tibiae are provided in Table 7.

Foot Three bones representing the foot are present: the left cuboid, left metatarsal V, and right metatarsal III (Fig. 11). On the left cuboid, the lateral facet for the sesamoid of peroneus longus is present, as is typical for cercopithecids. Metatarsal V preserves the proximal end, which articulates with the cuboid, but the shaft is broken and the distal end is not preserved. Metatarsal III is also broken, but the proximal half of the bone is preserved.

Systematic paleontology

Cercopithecidae gen. et sp. indet.

Referred material

KNM-TH 48374.

Horizon

Chemeron Formation outcrops, Tugen Hills, Kenya.

Localities/sites

Chemeron Formation BPRP #152, 2.63 Ma.

Description

KNM-TH 48374 The specimen KNM-TH 48374 is a fairly complete infant cercopithecid mandible, including the symphysis and both corpora. The rami are not preserved. Only one tooth is present, a worn right dp_3, which is a typical cercopithecid deciduous tooth with an elongated anterior portion. The anterior portion is particularly worn with no good discernable morphology; however, the distal half of the tooth appears to display quite columnar cusps (Fig. 12). Compared to the dp_3 described for *T. brumpti* from Koobi Fora (KNM-ER 2031) (Jablonski et al., 2008), the dp_3 here is much larger. Distal to the right dp_3, portions of the right m_1 appear visible in the broken crypt. The mandibular corpora are extremely thick, and much thicker than in KNM-ER 2031. The symphysis is also very thick and rugose with distinct mental ridges. A median mental foramen is present. On the lingual side of the symphysis, there is evidence of at least one large lingual mental foramen, but it is impossible to tell if other foramina may have been present.

Table 7
Tibial measurements in mm.

Measurement	Taxon (Specimen number)		
	T. brumpti (KNM-TH 46700, right)	*T. brumpti* (KNM-TH 46700, left)	*T. brumpti* (KNM-WT 39368)
Max length of tibia from tibial plateau to medial malleolus	195.5	X	219.4
AP diameter of the tibial plateau	29.9	31.1	X
ML diameter of the tibial plateau	40.9	40.1	X
PD distance from anterior margin of plateau to center of tuberosity	23.7	25.2	X
AP diameter at midshaft	19.8	20.0	(26.5)
ML diameter at midshaft	12.3	12.9	13.6
Relative tibial compression (AP diameter/ML diameter) × 100	161.0	155.0	(194.9)
AP diameter of distal epiphysis	20.9	X	X
ML diameter of distal epiphysis	24.3	X	X
PD length of malleolus	20.0	X	X

Notes: X = unavailable measurement. ML = medial–lateral; PD = proximal–distal; AP = anterior-posterior. Measurements for adult male *T. brumpti* KNM-WT 39368 taken from Jablonski et al. (2002). Numbers in parentheses represent estimates.

The specimen is not readily identifiable to a specific taxon, but it is quite intriguing contextually because it was found in association with the KNM-TH 46700 skeleton during preparation. Given a somewhat vertical orientation of the adult skeleton relative to the stratigraphy, the infant mandible is derived from the matrix just below the ribs, close to the cranium of the adult. Available measurements of KNM-TH 48374 are provided in Table 8.

Discussion

Previous analyses of *T. brumpti* postcrania have often made assignments to the species in the absence of definitive association; the partial skeleton here provides definitive associational context, and provides a confident assessment of female *T. brumpti* postcranial characters, particularly of the hindlimb. While a more comprehensive analysis of papionin postcranial morphology and variation is needed, the morphology preserved in KNM-TH 46700 combined with our own comparisons allows us to make some preliminary observations.

The pelvis of KNM-TH 46700 is relatively broad across the ilium, a feature shared with *Macaca*, *Cercocebus*, *Mandrillus*, and some *P. hamadryas* females. Fleagle and McGraw (2002) interpreted the distribution of this feature to indicate that a relatively wide ilium is a primitive feature among papionins and, if this is true, it appears that *T. brumpti* also retains this primitive feature. This stands in contrast to *T. gelada* and *T. oswaldi*, which exhibit the apparently derived condition of a relatively narrow ilium (Table 5; Fleagle and McGraw, 2002). This suggests that the *T. gelada* and *T. oswaldi* lineages may have evolved their narrow ilium independent of *Lophocebus* and *Papio*. A larger sample size of extant and fossil *Theropithecus* pelves will be necessary to appropriately evaluate this hypothesis.

For aspects of the lower limb, we did not observe some of the previously noted "typical" *T. brumpti* features on the KNM-TH 46700 skeleton (e.g., see Krentz, 1993a). The greater trochanter of the KNM-TH 46700 femur is curved proximo-medially, as in other *T. gelada* and *T. oswaldi* specimens, rather than a more proximal or vertical orientation as described and figured by Krentz (1993a). In addition, we could detect no pronounced reverse carrying angle *sensu* Krentz (1993a), or lateral angling of the femoral shaft onto the condyles. Instead, we only noticed a slight lateral excursion of the femoral shaft. This is perhaps surprising, since a distinct reverse carrying angle has been linked to the habitual squatting positional behavior of *T. gelada* and is also reported in specimens of *T. oswaldi* (Krentz, 1993a). Finally, the medial malleolus of the tibia does not

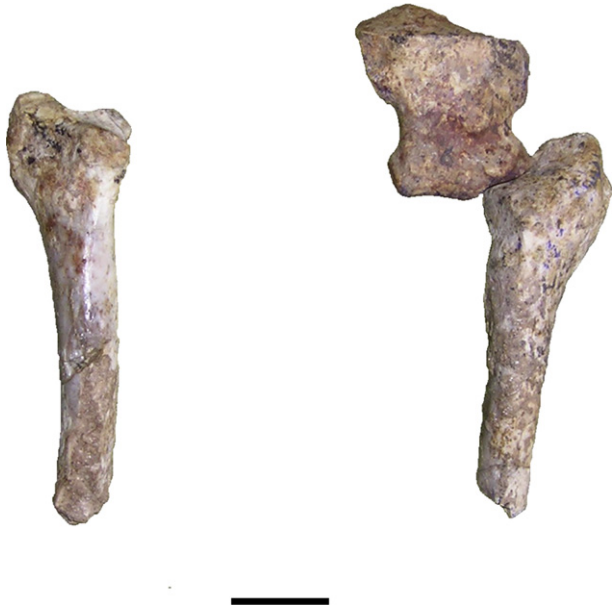

Figure 11. Foot bones of KNM-TH 46700. Left: right metatarsal III. Right: left cuboid and left metatarsal V. Scale = 1 cm.

Figure 12. The partial mandible of KNM-TH 48374. Top left: right lateral view. Top right: left lateral view. Bottom left: occlusal view. Bottom right: symphyseal view. Scale = 1 cm.

Table 8
Selected mandibular measurements of Cercopithecidae gen. et sp. indet. specimen KNM-TH 48374 in mm.

Specimen	Sex	Max sym height	Max sym depth	Corpus height at dP_3	Corpus width at dP_3	dP_3 MD	dP_3 MBL	dP_3 DBL
KNM-TH 48374	Indeterminate	15.0	11.0	15.0	7.0	9.7	5.1	5.4

Notes: Sym = symphyseal, MD = mesiodistal length, BL = buccolingual breadth, MBL = mesial buccolingual breadth, DBL = distal buccolingual breadth.

appear to be angled at 45° (*contra* Krentz, 1993a; Jablonski et al., 2002). Instead, the malleolus is most similar to modern *Papio* and displays little angulation in anterior and/or medial view.

These contrary descriptions could simply represent normal variation in the *T. brumpti* population during the East African Pliocene. They could also represent differences between males and females. However, other *Theropithecus* species are also sexually dimorphic, and no such differences have been reported between the sexes in these other taxa. It is also possible that the differences could be allometrically influenced, since female *T. brumpti* specimens are considerably smaller than males. Again, this possibility seems unlikely when considering that 1) no such differences have been reported among other dimorphic *Theropithecus* species, and 2) *T. gelada* is much smaller than *T. oswaldi* and *T. brumpti*, yet all three taxa have been argued to display the same features in the hindlimb (Krentz, 1993a). Another possibility is that some postcranial differences represent age-related variation, similar to the situation observed among craniodental features. Finally, since most of the postcranial elements from the Omo Shungura are isolated and unassociated with any *T. brumpti* craniodental material, it is possible that at least some of the hindlimb postcrania allocated to *T. brumpti* from the Omo are simply incorrectly assigned. Currently, it is impossible to choose between these alternatives, but future detailed studies of fossil papionin postcrania will hopefully be able to resolve the issue.

In addition to lacking key morphological features reported in other *T. brumpti* postcranial specimens, KNM-TH 46700 appears to be unique with regard to a couple of highly noticeable characters. To our knowledge, the large degree of antero-posterior bowing observed on the femoral shaft is not documented among other *T. brumpti* specimens and the possible functional reasons for this morphology are unclear. Similarly, the large degree of mediolateral bowing seen on the tibial shaft is also undocumented in other *T. brumpti* specimens, although we note its presence on geologically younger specimens of *T. oswaldi*. Again, while it is tempting to speculate that the mediolateral bowing is associated with squatting and shuffling, the functional demands associated with this type of bowing are currently unclear. The femur and the tibiae of KNM-TH 46700 do not appear to be distorted, so we consider it unlikely that these morphologies are simply due to postmortem deformation during the fossilization process.

The well-preserved skull of KNM-TH 46700 also displays a number of features not typically expressed, or expressed to a greater degree, in other known female crania. The anteriorly converging temporal lines and relatively strong nuchal crest for a female papionin extend the known variation for *T. brumpti* females, and these features are likely associated with the advanced age of KNM-TH 46700. In addition, the zygomatics are less flaring than those in *T. brumpti* females from the Omo Shungura Formation, such as the subadult female NME L32-155 or the adult female NME L122-34. However, both of these females appear to have been younger individuals than KNM-TH 46700. It is therefore possible that the degree of flare in the zygomatics is also an age-related characteristic. Another possibility is that variations in zygomatic flare are due to regional differences between the Omo Shungura *T. brumpti* population and the population of the Tugen Hills, two localities separated geographically by about 450 km. A specimen described from the geographically intermediate Koobi Fora Formation also displays weaker zygomatic arches compared to the Omo specimens, lending support to the notion that there was a large amount of variation in the *T. brumpti* population with regard to the degree of zygomatic arch flare (see also Eck and Jablonski, 1987). Given that there are few good female *T. brumpti* cranial specimens, it seems reasonable to expect that KNM-TH 46700 might extend known variation in *T. brumpti* female morphology.

Functionally, the features displayed in the lower limb of KNM-TH 46700 suggest an animal that moved in a way generally similar to that of modern savannah baboons (*Papio*). Features of the proximal femur such as the shortened neck (typical of *Theropithecus* in general), the extension of the articular surface onto the neck, the low angle of the neck, the large lesser trochanter, and the robust greater trochanter extending above the head suggest an increase in the efficiency of parasagittal movements at the hip joint and are common features of terrestrial quadrupeds. The shortened femoral neck and extension of the articular surface of the femoral head onto the neck may also indicate some degree of leaping or climbing ability (Fleagle, 1976; Krentz, 1993a). The distal femur and proximal tibia display features common to both arboreal and terrestrial quadrupeds, including asymmetrical condyles as well as asymmetrical and more rounded-to-prominent lips of the patellar groove. This last feature is similar to the condition observed in *Lophocebus* and *Papio*, which also possess a distal femur with relatively rounded lips of the patellar groove and a more prominent lateral lip (Fleagle and McGraw, 2002). The tibial shaft of KNM-TH 46700 is uncompressed, a similarity shared with extant *Papio*, *Lophocebus*, and *T. gelada* and in contrast with *Cercocebus* and *Mandrillus* (Fleagle and McGraw, 2002). The lack of a prominent medial lip of the patellar groove and the lack of tibial compression may suggest that vertical climbing was not a major component of this animal's locomotor repertoire.

In total, our reconstruction of the *T. brumpti* locomotor repertoire based on KNM-TH 46700 is broadly compatible with the general conclusions reached by previous authors (e.g., Krentz, 1993a; Jablonski et al., 2002, 2008). Thus, similar to other large terrestrially adapted papionins such as *Papio* baboons, *T. brumpti* was most likely a quadrupedal animal that spent most of its time on the ground but was also quite capable of moving adeptly within the trees. As a large papionin monkey found most often in environments reconstructed as forested (Eck and Jablonski, 1987), it is most likely that *T. brumpti* used arboreal supports to some degree (e.g., similar to modern *Papio* baboons). Because the forelimb of KNM-TH 46700 is not preserved, it is difficult to evaluate any competing hypotheses regarding the frequency of arboreal behaviors engaged in by *T. brumpti*, but there are no features of the hindlimb in KNM-TH 46700 that preclude some sort of arboreal capability. The absence of forelimb material associated with KNM-TH 46700 also makes it difficult to judge with confidence any potential differences in locomotor frequencies between the sexes in *T. brumpti*.

The lack of a pronounced reversed carrying angle of the femoral shaft and a highly angled tibial medial malleolus in KNM-TH 46700 is perhaps surprising, and it may suggest that *T. brumpti* did not engage in the same squatting and shuffling behaviors as frequently as extant geladas and as hypothesized for *T. oswaldi* (Krentz, 1993a). Alternatively, since the degree of distolateral excursion seen in extant geladas and KNM-TH 46700 overlaps with that seen among

modern *Papio* specimens, the functional significance of a slight reversed carrying angle is perhaps questionable. If other isolated femora that display more obvious reverse carrying angles truly represent *T. brumpti*, KNM-TH 46700 could simply demonstrate the normal range of variation in *T. brumpti* males or *T. brumpti* females.

In sum, it is unclear whether or not KNM-TH 46700 frequently engaged in the squatting and shuffling behavior typically observed in *T. gelada*. Given its specialized hand proportions, it would be particularly interesting if it did not. In this case, *T. brumpti* would retain the specialized hand morphology associated with modern gelada food gathering behaviors, but perhaps not the habitual squatting and shuffling locomotor behavior characterizing extant geladas. Additional and associated *T. brumpti* femora will be necessary to clarify the matter.

Lastly, KNM-TH 48374 represents an infant cercopithecid and was found in association near the ribs and cranium of KNM-TH 46700. Its overall robusticity, symphyseal rugosity, and relatively columnar distal cusps on the preserved dentition suggest that KNM-TH 48374 may represent a *T. brumpti* infant. However, given the lack of comparative material and the lack of a better-preserved dentition, we refrain from making a definitive assignment.

The reasons for the association of the infant mandible with the adult *T. brumpti* female are unclear. A number of entertaining and fanciful scenarios come to mind, ranging from the adult female unsuccessfully protecting her infant from the *Panthera* also found at the site, to predation on another monkey taxon, to infanticide. However, we have no evidence that BPRP #152 represents a catastrophic assemblage, and although intriguingly associated in the sediment, there is no reason whatsoever to believe these two individuals were ever associated in life. It is overwhelmingly more likely that this contextual oddity is nothing more than a coincidence, a chance association resulting from bone depositional processes at the site.

Conclusions

The partial skeleton of KNM-TH 46700 allows for a more detailed examination of *T. brumpti* female morphology. There appears to be a large amount of variation in *T. brumpti* female cranial morphology, particularly with respect to the degree of flare in the distinctive zygomatic arches. In contrast to specimens from the Omo Shungura Formation, KNM-TH 46700 expresses a weaker and less flaring zygomatic region. Preserved postcrania of KNM-TH 46700 include elements of the axial skeleton and lower limb. Previous descriptions of *T. brumpti* hindlimb morphology have noted a number of features not expressed in KNM-TH 46700, including a vertically oriented greater trochanter, a pronounced reversed carrying angle for the femoral shaft, and a tibial medial malleolus that is oriented at approximately 45°. It is unclear whether these differences represent general variation within the *T. brumpti* population, sexual dimorphism, or the incorrect assignment of previous hindlimb specimens to *T. brumpti*. Finally, the observable morphological features suggest that, similar to modern *Papio* baboons, KNM-TH 46700 was predominantly a terrestrial quadruped. As a large monkey most often associated with forested environments, it is also likely that *T. brumpti* was capable of moving in the trees. From the available evidence, it is unclear whether or not KNM-TH 46700 frequently engaged in the specialized squatting and shuffling behavior observed in extant geladas.

Acknowledgements

This research forms part of the work of the *Baringo Paleontological Research Project* (BPRP) based at Yale University, and was carried out in collaboration with the National Museums of Kenya. We thank the Government of the Republic of Kenya for permission to carry out research in Kenya (Permit MOHEST/13/001/C 1391/ issued to AH), and permission to excavate from the Minister for Home Affairs and National Heritage. Eileen Westwig kindly provided access to extant primate comparative material housed at the AMNH. We thank Mauricio Antón for permission to modify and use his artwork in Fig. 4. This study was kindly supported by a Donnelley Fellowship from the Yale Institute for Biospheric Studies to CCG, and by the MacMillan Center for International and Area Studies, the John F. Enders Fellowship, both from Yale University, and the Bryan Patterson Memorial Grant from the Society of Vertebrate Paleontology to EDG. BPRP has been supported by grants to AH from NSF (currently #BSC-071137 with JK and Alan Deino), and also from Clayton Stephenson, and the Schwartz Family Foundation. Fieldwork during the season in which the skeleton was found was supported by an Emory URC grant to JK. We are grateful to Bonface Kimeu and Julius Kleria for their part in the discovery and for considerable help with fieldwork, and to Bonface Kimeu for laboratory assistance. The skeleton was prepared by Bonface Kimeu and by Christopher Kiarie. Laura Bishop kindly discussed pigs with us, and Faysal Bibi proffered words of advice on a bovid. The National Museums of Kenya provided valuable logistical support, and we thank particularly Emma Mbua, Head of the Division of Earth Sciences. EDG thanks Andrew Goble for his assistance. Finally, CCG thanks David McKenzie and Sarah Band for their wonderful and enduring hospitality while in Nairobi.

References

Andrews, C.W., 1916. Note on a new baboon (*Simopithecus oswaldi*, gen. et sp. nov.) from the Pliocene of British East Africa. Ann. Mag. Nat. Hist 18, 410–419.

Arambourg, C., 1947. Mission scientifique de l'Omo (1932–1933), vol. 1, fasc. 3: Geologie, Anthropologie. Museum National d'Histoire Naturelle, Paris.

Bishop, L.C., Hill, A., Kingston, J.D., 1999. Palaeoecology of suidae from the Tugen Hills, Baringo, Kenya. In: Andrews, P., Banham, P. (Eds.), Late Cenozoic Environments and Hominid Evolution: a Tribute to Bill Bishop. Geological Society of London, London, pp. 99–111.

Broom, R., 1937. On some new Pleistocene mammals from limestone caves of the Transvaal. S. Afr. J. Sci. 33, 750–768.

Broom, R., Jensen, J.S., 1946. A new fossil baboon from the caves at Potgietersrust. Ann. Trans. Mus. 20, 337–340.

Broom, R., Hughes, A.R., 1949. Notes on the fossil baboons of the Makapan caves. S. Afr. J. Sci. 2, 194–196.

Broom, R., Robinson, J.T., 1949. A new type of fossil baboon, *Gorgopithecus major*. Zool. Soc. Lond. 119, 374–383.

Buettner-Janusch, J., 1966. A problem in evolutionary systematics: nomenclature and classification of baboons, genus *Papio*. Folia Primatol. 4, 288–308.

Burnett, G.T., 1828. Illustrations of the Manupeda or apes and their allies: being the arrangement of the Quadrumana or Anthropomorphous beasts indicated in the outline. Quart. J. Sci. Lit. Art 26, 300–307.

Ciochon, R.L., 1993. Evolution of the Cercopithecoid forelimb: phylogenetic and functional implications from morphometric analyses. U.C. Pub. Geol. Sci. 138, 1–251.

Deino, A.L., Hill, A., 2002. $^{40}Ar/^{39}Ar$ dating of the Chemeron Formation strata encompassing the site of hominid KNM-BC 1, Tugen Hills, Kenya. J. Hum. Evol. 42, 141–151.

Deino, A., Kingston, J., Glen, J.M., Edgar, R.K., Hill, A., 2006. Precessional forcing of lacustrine sedimentation in the late Cenozoic Chemeron Basin, central Kenya Rift, and calibration of the Gauss/Matuyama boundary. Earth Planet Sci. Lett. 247, 41–60.

Deino, A.L., Tauxe, L., Monaghan, M., Hill, A., 2002. $^{40}Ar/^{39}Ar$ geochronology and paleomagnetic stratigraphy of the Lukeino and lower Chemeron succession at Tabarin and Kapcheberek, Tugen Hills, Kenya. J. Hum. Evol. 42, 117–140.

Delson, E., 1993. *Theropithecus* fossils from Africa and India and the taxonomy of the genus. In: Jablonski, N.G. (Ed.), *Theropithecus*: The Rise and Fall of a Primate Genus. Cambridge University Press, Cambridge, pp. 157–189.

Delson, E., Terranova, C.J., Jungers, W.L., Sargis, E.J., Jablonski, N.G., Dechow, P.C., 2000. Body mass in Cercopithecidae (Primates, Mammalia): estimation and scaling in extinct and extant taxa. Anthropol. Pap. Am. Mus. Nat. Hist. 83, 1–159.

Eck, G.G., Howell, F.C., 1982. Un primate des formations plio-pléistocènes d'Afrique oriental: *Theropithecus brumpti* (*Arambourg*), (Primates, Cercopithecidae). C.R. Acad. Sci. Paris 295, 397–400.

Eck, G.G., Jablonski, N.G., 1984. A reassessment of the taxonomic status and phyletic relationships of *Papio baringensis* and *Papio quadratirostris*. Am. J. Phys. Anthropol. 65, 109–134.

Eck, G.G., Jablonski, N.G., 1987. The skull of *Theropithecus brumpti* compared with those of other species of the genus *Theropithecus*. In: Coppens, Y., Howell, F.C.

(Eds.), Les Faunes Plio-Pleistocenes de la Basse Vallee de l'Omo (Ethiopie), Tome 3, Cercopithecidae de la Formation Shungura. Cahiers de Paleontologie, Editions du Centre National de la Recherche Scientifique, pp. 11–122.
Erxleben, J.C.P., 1777. Systema regni animalis…Classis 1, Mammalia. Weygand, Lipsiae.
Fleagle, J.G., 1976. Locomotor behavior and skeletal anatomy of sympatric Malaysian leaf monkeys (*Presbytis obscura* and *Presbytis melalophos*). Yearbk. Phys. Anthropol. 20, 440–463.
Fleagle, J.G., McGraw, W.S., 2002. Skeletal and dental morphology of African papionins: unmasking a cryptic clade. J. Hum. Evol. 42, 267–292.
Freedman, L., 1957. The fossil Cercopithecoidea of South Africa. Ann. Trans. Mus. 23, 121–262.
Frost, S.R., Delson, E., 2002. Fossil Cercopithecidae from the Hadar Formation and surrounding areas of the Afar Depression, Ethiopia. J. Hum. Evol. 43, 687–748.
Geoffroy, E., 1812. Tableau des quadrumanes, 1. Ord. Quadrumanes. Ann. Mus. Hist. Nat. Paris 19, 85–122.
Geoffroy Saint-Hilaire, I., 1843. Description des mammifères nouveaux ou imparfaitement connus…Famille des Singes. Arch. Mus. Hist. Nat. Paris 2, 486–592.
Gilbert, C.C., 2007. Craniomandibular morphology supporting the diphyletic origin of mangabeys and a new genus of the *Cercocebus/Mandrillus* clade, *Procercocebus*. J. Hum. Evol. 53, 69–102.
Gilbert, C.C., 2008. African papionin phylogenetic history and Plio-Pleistocene biogeography. Ph.D. dissertation, Stony Brook University.
Gilbert, C.C., 2009. Phylogenetic history of the African papionins: a cladistic analysis of extant and fossil taxa using craniodental data. Am. J. Phys. Anthropol. 48S, 198.
Gilbert, C.C., Frost, S.R., Strait, D.S., 2009. Allometry, sexual dimorphism, and phylogeny: a cladistic analysis of extant papionins using craniodental data. J. Hum. Evol. 57, 298–320.
Goble, E., Hill, A., Kingston, J.D., 2008. Digital elevation models as heuristic tools. PaleoAnthropology 2008, A9.
Gray, J.E., 1821. On the natural arrangement of vertebrate animals. Lond. Med. Repository Record 15, 296–310.
Gray, J.E., 1843. List of the Specimens of Mammalia in the Collection of the British Museum. British Museum, London.
Harris, J.M., Cerling, T.E., 2002. Dietary adaptations of extant and Neogene African suids. J. Zool. Lond. 256, 45–54.
Hill, A., 2002. Paleoanthropological research in the Tugen Hills, Kenya. J. Hum. Evol. 42, 1–10.
Jablonski, N.G., 1986. The hand of *Theropithecus brumpti*. In: Else, J.G., Lee, P.C. (Eds.), Primate Evolution: Proceedings of the 10th Congress of the International Primatological Society, vol. 1. Cambridge University Press, Cambridge, pp. 173–182.
Jablonski, N.G., 1993a. The phylogeny of *Theropithecus*. In: Jablonski, N.G. (Ed.), *Theropithecus*: The Rise and Fall of a Primate Genus. Cambridge University Press, Cambridge, pp. 209–224.
Jablonski, N.G., 1993b. The evolution of the masticatory apparatus in *Theropithecus*. In: Jablonski, N.G. (Ed.), *Theropithecus*: The Rise and Fall of a Primate Genus. Cambridge University Press, Cambridge, pp. 299–329.
Jablonski, N.G., 1994. Convergent evolution in the dentitions of grazing macropodine marsupials and the grass-eating cercopithecine primate *Theropithecus gelada*. J. Roy. Soc. W. Aust. 77, 37–43.
Jablonski, N.G., 2002. Late Neogene cercopithecoids. In: Hartwig, W.C. (Ed.), The Primate Fossil Record. Cambridge University Press, Cambridge, pp. 255–299.
Jablonski, N.G., Leakey, M.G., Antón, M., 2008. Systematic paleontology of the cercopithecines. In: Jablonski, N.G., Leakey, M.G. (Eds.), Koobi Fora Research Project Volume 6: The Fossil Monkeys. California Academy of Sciences, San Francisco, pp. 103–300.
Jablonski, N.G., Leakey, M.G., Kiarie, C., Antón, M., 2002. A new skeleton of *Theropithecus brumpti* (Primates: Cercopithecidae) from Lomekwi, West Turkana, Kenya. J. Hum. Evol. 43, 887–923.
Jolly, C.J., 1972. The classification and natural history of *Theropithecus (Simopithecus)* (Andrews, 1916), baboons of the African Plio-Pleistocene. Bull. Br. Mus. (Nat. Hist.) Geol. 22, 1–123.
Kingston, J., 1999. Environmental determinants in early hominid evolution: issues and evidence from the Tugen Hills, Kenya. In: Andrews, P., Banham, P. (Eds.), Late Cenozoic Environments and Hominid Evolution: a Tribute to Bill Bishop. Geological Society of London, London, pp. 69–84.
Kingston, J., Deino, A., Edgar, R.K., Hill, A., 2007. Astronomically forced climate change in the Kenyan Rift Valley 2.7–2.55 Ma: implications for the evolution of early hominin ecosystems. J. Hum. Evol. 53, 487–503.
Kitching, J.W., 1952. A new type of fossil baboon: *Brachygnathopithecus peppercorni*, gen. et sp. nov. S. Afr. J. Sci. 49, 15–17.
Krentz, H., 1993a. Postcranial anatomy of extant and extinct species of *Theropithecus*. In: Jablonski, N.G. (Ed.), *Theropithecus*: The Rise and Fall of a Primate Genus. Cambridge University Press, Cambridge, pp. 383–422.
Krentz, H., 1993b. The forelimb anatomy of *Theropithecus brumpti* and *Theropithecus oswaldi* from the Shungura Formation, Ethiopia. Ph.D. dissertation, University of Washington.
Leakey, M.G., 1993. Evolution of *Theropithecus* in the Turkana Basin. In: Jablonski, N.G. (Ed.), *Theropithecus*: The Rise and Fall of a Primate Genus. Cambridge University Press, Cambridge, pp. 85–123.
Leakey, R.E.F., 1969. New Cercopithecidae from the Chemeron Beds of Lake Baringo, Kenya. In: Leakey, L.S.B. (Ed.), Fossil Vertebrates of Africa, vol. 1. Academic Press, London, pp. 53–70.
Linnaeus, C., 1758. Systema naturae per regna tria naturae, secundum classes, ordines genera, species cum characteribus, differentris, synonymis, locis. Tomus 1, Editis decima, reformata. Laurentii Salvii, Stockholm.
McGraw, W.S., Fleagle, J.G., 2006. Biogeography and evolution of the *Cercocebus-Mandrillus* clade: evidence from the face. In: Lehman, S.M., Fleagle, J.G. (Eds.), Primate Biogeography: Progress and Prospects. Springer, New York, pp. 201–224.
Mivart, St. G., 1864. Notes on the crania and dentition of the Lemuridae. Proc. Zool. Soc. Lond. 1864, 611–648.
Napier, J.R., Napier, P.H., 1967. A Handbook of Living Primates. Academic Press, London.
Rüppell, E., 1835. Neue Wirbeltiere zuder Fauna von Abyssinien gehorig. In: Säugetiere, vol. 1. Schmerber, Frankfurt.
Smith, R.J., Jungers, W.L., 1997. Body mass in comparative primatology. J. Hum. Evol. 32, 523–559.
Strasser, E., 1992. Hindlimb proportions, allometry, and biomechanics in Old World Monkeys (Primates, Cercopithecidae). Am. J. Phys. Anthropol. 87, 187–213.
Szalay, F.S., Delson, E., 1979. Evolutionary History of the Primates. Academic Press, New York.
Vram, U.G., 1922. Sul genere *Theropythecus*. Arch. Zool. Italiano 10, 169–214.